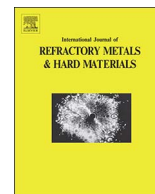




Contents lists available at ScienceDirect

# International Journal of Refractory Metals & Hard Materials

journal homepage: [www.elsevier.com/locate/IJRMHM](http://www.elsevier.com/locate/IJRMHM)

## Plastic deformation of recrystallized tungsten-potassium wires: Constitutive deformation law in the temperature range 22–600 °C



D. Terentyev<sup>a,\*</sup>, J. Riesch<sup>b</sup>, S. Lebediev<sup>c</sup>, T. Khvan<sup>c</sup>, A. Zinovev<sup>a,d</sup>, M. Rasiński<sup>e</sup>, A. Dubinko<sup>a</sup>, J.W. Coenen<sup>e</sup>

<sup>a</sup> Structural Materials Group, Institute of Nuclear Materials Science, SCK-CEN, Mol 2400, Belgium

<sup>b</sup> Max-Planck-Institut für Plasmaphysik, 85748 Garching, Germany

<sup>c</sup> V.N. Karazin Kharkiv National University, 4 Svobody Sq., Kharkiv 61022, Ukraine

<sup>d</sup> iMMC, Université catholique de Louvain, Louvain-la-Neuve 1348, Belgium

<sup>e</sup> Forschungszentrum Jülich GmbH, Institut für Energie- und Klimaforschung – Plasmaphysik, Partner of the Trilateral Euregio Cluster (TEC), 52425 Jülich, Germany

### ARTICLE INFO

#### Keywords:

Tungsten  
Tungsten wire  
Plasticity  
Potassium doped

### ABSTRACT

Recent efforts dedicated to the mitigation of tungsten (W) brittleness have demonstrated that tungsten fiber-reinforced composites acquire extrinsic toughening even at room temperature, which is due to the outstanding strength of W wires. However, high temperature operation/fabrication of the fiber-reinforced composite might result in the degradation of the mechanical properties of W wires. To address this, we investigate mechanical and microstructural properties of potassium-doped tungsten wires, being heat treated at 2300 °C and tested in temperature range 22–600 °C. Based on the microscopic analysis, the engineering deformation curves are converted into actual stress - strain dataset, accounting for the local necking. The analysis demonstrates that local strain in the necking region can reach up to 50% and the total elongation monotonically increases with temperature, while the ultimate tensile strength goes down. Preliminary transmission electron microscopy analysis using FIB-cut lamella from the necking region revealed the presence of curved dislocation lines in the sample tested at 300 °C, proving that plastic deformation occurred by dislocation glide.

### 1. Introduction

Tungsten (W) is currently the main candidate material for the first wall of a fusion reactor as it is resilient against erosion and exhibits low tritium retention as well as a very high melting point and a good thermal conductivity [1]. However as a typical bcc metal, tungsten features intrinsic brittleness up to a temperature of about 200–300 °C [2, 3] and up to above 900 °C after the annealing at high temperature [4]. In addition, W is prone to operational embrittlement e.g. by grain coarsening [5] or/and neutron irradiation [6].

Extensive work has been done to qualify current materials with respect to these issues for ITER. This is especially true for W used as the first wall and divertor material (see [1, 7, 8] and references therein). For the next step devices, e.g. DEMO, or a future fusion reactor the limits on power exhaust, availability and lifetime are quite more stringent. Extensive studies and material programs [9–11] have already been performed hence it is assumed that the boundary conditions [12] to be fulfilled for the materials are in many cases exceed the technical feasibility limits as set today. Efforts to establish new advanced options

for plasma-facing material/components are moving forward focusing on crack resilient materials with low activation, minimal tritium uptake, long lifetime and low erosion. The operational gap (~350–600 °C) between materials for cooling structures e.g. Cu, and the plasma-facing materials needs to be bridged as well [7, 13].

Tungsten fiber-reinforced composites ( $W_f/W$ ) overcome the brittleness problem of bulk tungsten by utilizing extrinsic toughening mechanisms similar to ceramic matrix composites [14]. The proof of extrinsic toughening in such a composite system has been shown in the past years at the Max-Planck-Institute for Plasma Physics, Garching (IPP) [15].  $W_f/W$  composites consist of tungsten fibers made of commercially drawn tungsten wire embedded in a tungsten matrix produced either by a chemical process [16] or by powder metallurgy [17].

The structural integrity of  $W_f/W$  composites are based on the exceptional properties of the tungsten wire used as fiber reinforcement: pure as well as potassium doped tungsten wire shows exceptional ductility [18] and very high strength [19] even at room temperature in contrast to conventional bulk tungsten being brittle at room temperature [2]. These are ideal properties facilitating the toughening of  $W_f/W$

\* Corresponding author.

E-mail address: [dterenty@sckcen.be](mailto:dterenty@sckcen.be) (D. Terentyev).

as the high strength is important for the bridging effect and ductile deformation allows the dissipation of a substantial amount of energy [20]. This success gave a push to study properties of the tungsten wire solely, and in particular investigation of the mechanical response at elevated temperatures.

Recently, a set of W wires with and without potassium doping was studied in [21] by mechanical tests performed up to 600 °C. For the as-drawn wire, the potassium doping practically did not change the response to the mechanical load. The fracture occurred by the elongation and delamination of sub-grains (elongated in the direction of wire axis) showing the knife-edge necking fracture typically observed for W wire [22]. Both fracture stress and fracture strain monotonically decreased with increasing the test temperature. The necking was essentially localized, and the length of a neck was about 150–200 μm being comparable with the initial diameter of the wire. No diffuse necking process occurred during the deformation of the wire in the as-fabricated condition.

2300 °C annealed potassium-doped wire was seen to have much lower yield and fracture stress. The fracture mechanism was also different, namely: cleavage at 100 °C and ductile necking above 300 °C. The change of the deformation mechanism and thereby increased elongation was attributed to the onset of the 3D plastic deformation by movement of screw dislocations. The total elongation of the wire before the fracture was much higher as compared to the as-drawn wires, moreover the plastic deformation was more pronounced, as revealed by post mortem microscopic study. Hence, the understanding of the local deformation and extraction of the post-necking stress-strain characteristics of the annealed wire is needed to complete this work.

In the following, we continue our study and perform microstructural analysis of the deformed fibers to deduce geometric parameters of the necked regions and reconstruct the post-necking stress – strain (PNSS) relationship thus extracting the constitutive law. The results are then summarized in a convenient format to be used by a conventional finite element code (e.g. Abaqus) to model plastic deformation of the fibers.

## 2. Experimental details

Drawn potassium doped (60–75 ppm) tungsten wire, similar to the wire used in [21, 23] was provided by the OSRAM GmbH, Schwabmünchen. The diameter of the doped wire was measured to be  $148.7 \pm 0.2 \mu\text{m}$  [23]. Measurements were performed by high resolution optical microscope. The K-doped wire was cut into pieces of 100 mm and these were annealed at 2300 °C. To perform the annealing, the wire was straightened prior to cutting. The straightened and cut wire pieces were then annealed in a tube furnace under hydrogen atmosphere at OSRAM GmbH. During this process the samples were placed on a shovel (carbon free) and kept at 2300 °C for 30 min.

In order to clamp, the ends of the wire pieces (called fibers in the following) were clutched by two parallel mirror-polished stainless steel plates by applying the minimum force required to carry out the mechanical test and avoid deformation near the clamping plates or sliding of the wires between the plates. The gauge section was 30 mm. The sample holder was equipped with a guide rail to ensure perfect alignment. More details about testing procedure can be found in our recent work [21].

To ensure constant temperature during the test, the gauge section of the sample and inner parts of the holders were placed inside a cylindrical furnace. The temperature of the sample was measured by a thermocouple, connected to a digital voltmeter. Accuracy of the temperature measurement was ~1 K. The sample were tested in air. Prior to proceed with the loading, the system was equilibrated at the desired test temperature for 30 mins.

The deformation on the sample is applied via a pull rod driven by an electrical gear box, with a maximum load of 0.2 kN. A constant displacement rate with a cross-head speed of 5 μm/s was applied until fracture. The load, measured by a strain gauge, was registered with a

frequency of 0.3 Hz. The initial and final (i.e. after fracture) length of each sample was determined by the horizontal optical comparator with a precision of 1 μm.<sup>1</sup> The relative error on the measurement of the pull rod displacement is ± 0.1% and the absolute error on the stress measurement (for the strain region where the cross-section of the fiber remains constant) is 15 MPa.

After the test, the surface of the fractured samples was inspected by SEM on both ends. This allowed one to clarify the morphology of the fracture surface and assist the discussion on the deformation mode. The employed scanning electron microscope was a JEOL JSM-6610LV (JEOL, Tokyo, Japan) and operating conditions employed 20 kV accelerating voltage and 12–20 mm working distance. All SEM images presented in this work were acquired using a secondary electron (SE) detector. The necking region of each fractured sample was investigated in an optical microscope (Leica) to obtain the necking geometry, needed to reconstruct the stress – strain relationship in the post-necking region accounting for the non-uniform reduction of the wire cross-section. The necking diameter was also measured using SEM to refine/validate the measurements done by the optical microscope. The methodology used to convert the engineering stress-strain into actual stress-strain data is described in the following section, following the presentation of the engineering data.

## 3. Results and discussion

The test matrix is given in Table 1. At least five valid tests per condition were performed. Here, we provide examples of stress-strain curves and micrographs of few selected fibers.

Fig. 1(a) collects typical stress-strain curves obtained for the fibers tested at different temperatures. At room temperature, the wire does not show any yield and breaks in the elastic mode of the deformation, hence we have not included it in the figure. The low-strain deformation region is shown in Fig. 1(b) to illustrate that the irreversible plastic deformation begins before the engineering strain reaches 0.2% (indicated by a dashed line). The deflection from the straight line (i.e. purely elastic deformation) emerges around 0.005–0.01% deformation strain. One can also clearly see the presence of the yield drop. In fact, the yield drop was registered in all the samples, but its amplitude decreases with the test temperature and is therefore not visible for the higher temperature curves. The “yield drop” is likely to be associated with the presence of interstitial impurities [24], mostly carbon. At this point, it is impossible to identify the actual mechanism responsible for the observed yield drop unambiguously. It is known that the wires were drawn from the technically pure W which contained at least few tens of ppm of carbon. The thermal annealing was performed 2300 °C, and should have resulted in the removal of the most of grain boundary interfaces as well as dislocation networks. While potassium is expected to remain in clusters (precipitates) not being dissolved in the matrix. Correspondingly, the retained interstitial carbon atoms might have rearranged to segregate at the remaining dislocations and grain boundaries, overall resulting in the suppression of the dislocation glide/emission causing the occurrence of the upper and lower yield point.

For the wires tested at 100 and 200 °C, the maximum engineering stress was reached shortly after the deformation strain reached about 0.005–0.01%, and therefore we use this level as the onset of the diffuse necking and recalculate the actual stress and strain, as explained below. If the particular test does not demonstrate diffuse necking, 0.2% of engineering strain is taken as the onset of the plastic deformation, as for instance is the case for 500 °C test in Fig. 1.

Once the maximum engineering stress is reached, we assume that the necking process onsets and then only the local region of the wire experiences plastic deformation (indicated by black arrows in Fig. 2).

<sup>1</sup> The fiber ends are placed in the special bed, where one end is abut and the length is measured by optical microscopy.

Download English Version:

<https://daneshyari.com/en/article/7989603>

Download Persian Version:

<https://daneshyari.com/article/7989603>

[Daneshyari.com](https://daneshyari.com)